



Evaluation and optimization of dielectric strength of porcelain insulators containing Cattle Bone Ash as a fluxing material

Ritah Abindabyamu^a, John Paul Eneku^b, William Ochen^{a,*} 

^a Department of Physics, Kyambogo University P.O Box 1, Kyambogo, Uganda

^b Department of Physics, Makerere University P.O Box 7076, Kampala, Uganda

ARTICLE INFO

Editor: Mohamed Fathy El-Amin Mousa

Keywords:

Voltage breakdown
Response surface method
Anorthite
Flexural strength
Electrical insulators

ABSTRACT

Environmental pollution from cattle bones has been a major concern of recent. Cattle bones when calcinated at 700 °C decompose into lime (CaO) and β -tricalcium Phosphate [$\text{Ca}_3(\text{PO}_4)_2$]. CaO has fluxing behavior similar to Na_2O and K_2O found in feldspar. This study aimed at investigating the dielectric and mechanical properties of porcelain insulators containing cattle bone ash (CBA) as a replacement for feldspar. CBA at 0 wt%, 5 wt%, 10 wt%, 20 wt% and 25 wt% were added. The samples were pressed at 40 MPa and fired at 1000-1250 °C. The microstructure and phase analysis of the samples was carried out using scanning electron microscope and X-ray diffraction method respectively. Response surface method (RSM) was used to optimize the dielectric strength of the samples. The results revealed that in samples with 25 wt% CBA, a maximum dielectric strength of 15 kV/mm was achieved at 1000 °C. However, in samples with 0 wt% CBA, a dielectric strength of 15 kV/mm was obtained at 1250 °C. In addition, the optimal dielectric strength of 13 kV/mm using RSM was achieved at 1040 °C. The results indicate that adding CBA lowers the firing temperature by approximately 250 °C. Firing temperature in this case was the temperature when the dielectric strength was maximum. The low firing temperature was attributed to the high content of CaO (71%) in CBA. In all the samples with CBA, the dielectric strength of 6-15 kV/mm achieved was within the specification for porcelain insulators. Therefore, CBA can be used to replace feldspar in the production of porcelain insulators.

Introduction

Electrical insulators are materials without free electrons therefore, they resist the flow of electric current. Electrical insulators can be classified as high voltage or low voltage insulators. High voltage insulators are designed for systems with over 1 kV [1]. Low voltage insulators are used when the voltage required is below 1 kV. Insulators are important in the generation, transmission and distribution of electricity from the power stations to the consumers [2]. They are used to isolate conductors from towers and also to provide mechanical support for conductor lines during the transmission or distribution process. Therefore, they must exhibit high mechanical strength, low loss factor and high dielectric strength in corrosive and humid conditions [3].

Electrical insulators can be made from polymers, glasses, or porcelain materials. Polymeric insulators are lightweight and they inhibit flashovers induced by contaminations such as dust, fog and soluble salts (NaCl) more effectively than glass and porcelain insulators. However, due to low hydrophobicity, polymeric insulators experience discharge currents leading to early failure [4,5].

* Corresponding author.

E-mail address: wocen@kyu.ac.ug (W. Ochen).

<https://doi.org/10.1016/j.sciaf.2026.e03428>

Received 30 January 2026; Received in revised form 8 May 2026; Accepted 24 May 2026

Available online 26 May 2026

2468-2276/© 2026 The Author(s). Published by Elsevier B.V. This is an open access article under the CC BY-NC-ND license (<http://creativecommons.org/licenses/by-nc-nd/4.0/>).

Glass insulators have long life under dielectric stress than polymeric materials. Glass insulators however are susceptible to cracks due to thermal stresses and lightning strikes. The presences of cracks act as conductive path ways for current, causing voltage breakdown. Porcelain insulators can withstand stresses due to switching under normal load and over voltage load, under abnormal environment [3].

The global demand for electricity has increased in the past decades, and it is anticipated to increase in future. In 2015, the world net electricity consumption was 18,453 billion kWh representing a 12.8% increase compared to 2010. The global electricity consumption reached 23,072 billion kWh in 2025 which was an increase of 11.5% compared to 2020, and it is anticipated to increase by 57% in 2040 [1,6]. The increase was driven by population growth, industrialization and urbanization [7]. Efficient distribution of electricity requires insulating materials. The dielectric and mechanical strength of the insulating materials are crucial [1]. The dielectric strength of the insulator determines its ability to withstand high voltage without breaking down. The mechanical strength defines its ability to withstand harsh conditions without failure. Porcelain insulators are known to have a mechanical strength of greater than 35 MPa and dielectric strength of more than 6 kV/mm [1,8,9]. They are preferably used for high and low voltage applications in generation, transmission and distribution networks [10].

Porcelain insulators are made from a triaxial mixture of clay, feldspar and sand. These materials are mixed in ratios of 50% clay, 25% feldspar, and 25% sand [8,11]. The clay component of the mixture constitutes kaolin and ball clay. Kaolin is the main source of alumina and when fired it reacts with silica to form mullite fibers. The presence of mullites enhances the dielectric and mechanical strength of porcelain insulators [11]. Ball clay eases shaping of the body by providing plasticity to the mixture. Sand is a filler material, it maintains the dimensional stability of the fired body [12]. Feldspar is used to lower the firing temperature of the kiln. This is attributed to the presence of fluxing oxides such as Na_2O , K_2O , MgO , CaO and MnO in feldspar [9,11]. These oxides foster vitrification through liquid phase sintering mechanism. The optimal sintering temperature of porcelain insulators containing feldspar as a fluxing materials is in a range of 1200-1300°C [1,13]. The relatively high temperatures affect industrial production because it contributes to high energy consumption. Therefore, there is need to explore alternative flux materials.

Research on the production of porcelain insulators using recycled waste materials has gained attention in recent years [9,14,15]. Belhouchet et al. [14] developed electrical porcelain insulators by replacing feldspar with recycled waste glass in ratios of 0 wt%, 10 wt%, 20 wt% and 30 wt%. The authors reported improved values of mechanical (Vickers micro hardness) and dielectric behavior (dielectric loss factor and dielectric loss tangent) when 20 wt% of feldspar was replaced with recycled glass waste before firing at 1000-1100 °C. A similar study by Tullu et al. [9] reported optimal results of dielectric strength (8.9 kV/mm) when 10 wt% cullets was added to 45 wt% clay, 35 wt% feldspar and 10 wt% quartz and then sintered at 1200 °C. Shanmugam et al. [15] elaborated porcelain insulators using bamboo leaf ash (BLA) as a replacement for quartz. The samples exhibited better mechanical and dielectric properties than the commercial insulators when 10 wt% of BLA was added before sintering at 1250 °C. Related works can be found in refs. [16–18]. To the author's knowledge, there are limited trials to recycle cattle bones for use as a fluxing agent in porcelain insulators.

The population of cattle in Uganda is on the rise, and the bones have no commercial use. Instead, they are dumped in landfills causing economic and environmental challenges. The bones are known to contain calcium which is an ingredient responsible for bone formation, and bone mass maintenance [19]. Cattle bones decompose into β -tricalcium Phosphate [$\text{Ca}_3(\text{PO}_4)_2$], and lime (CaO) at a calcination temperature of 700 °C and above to produces 61-78 % CaO [20,21]. As mentioned earlier, CaO has fluxing behavior and therefore, it can lower the vitrification temperature through liquid phase sintering mechanism. This work, intended to use cattle bone ash (CBA) in a range of 0-25 wt% (see supplementary Table 1) as a replacement of feldspar in the production of porcelain insulators hitherto not tried before. The mechanical and dielectric strength of the insulators was analyzed. The Response Surface Method (RSM) implemented using design expert software version 13 was used to evaluate the statistical significance of the factors (CBA ratio and firing temperature) on the responses (dielectric and flexural strength), and to optimize the responses. Further, phase and micro-structure analysis of the insulators was carried out at various temperatures using scanning electron microscope (SEM) and X-ray diffractometer (XRD) respectively.

Table 1
Chemical composition (%) of the starting raw materials.

Oxides	Cattle bone ash	Ball clay	Feldspar	Sand	Kaolin
SiO_2	16.15	65.46	68.02	85.79	62.53
Fe_2O_3	0.11	13.06	2.80	0.73	2.96
Al_2O_3	-	10.15	8.21	10.97	28.33
CaO	71.02	8.07	0.93	-	5.34
MnO_2	0.42	0.43	0.39	0.47	0.01
K_2O	0.16	0.18	19.18	1.55	0.23
NiO_2	2.13	-	-	-	-
MgO	1.01	-	-	-	-
TiO_2	-	2.02	-	-	-
P_2O_5	-	0.24	0.22	0.29	0.32
Na_2O	1.36	-	-	-	-
LOI	6.82	0.51	0.20	0.10	0.87
Total	99.18	100.10	99.94	99.91	98.29

Materials and methods

Location of deposits

The raw materials used in this study were sourced from the deposits found in Uganda. Kaolin and feldspar were sourced from Mutaka in Bushenyi District which is 340 km West of Kampala City. Mutaka is located on Latitude 0°32'11.39"N and Longitude 30°11'3.60" E. Ntawo deposit in Mukono District provided ball clay, it is located at Latitude 0°14'60.00" N and Longitude 32°54'59.99" E. The cattle bones were collected from Kampala City abattoir which is found at Old Port-bell road on Latitude 0°17'14.40" N and Longitude 32°39'8.99" E. Sand was obtained from Lido beach in Wakiso District which is about 48 km from Kampala City on Latitude 0°3'10.02"N and Longitude 32°27'54E. The chemical composition of the raw materials was determined using X-ray fluorescence method and the results are shown in [Table 1](#).

Material processing

The clay was soaked in water to allow the impurities to settle at the bottom of the container. The suspension was wet sieved and dried under direct sunlight. The clay was milled using lake stones as the grinding medium. The milled clay was dry sieved using a 90 µm mesh. Sand was washed with water to remove the impurities. It was pulverized using a planetary ball mill (Retsch PM 100) running at 200 rpm. Steel balls of 14 mm equal diameter were used as the grinding medium. The milled sand was sieved using a 90 µm mesh sieve. Kaolin was mined and dry sieved using 90 µm mesh sieve. Feldspar rocks were crashed using a hammer, dry milled and sieved using a 90 µm mesh sieve. Cattle bones were boiled in water to remove the flesh, washed with water and sun dried to remove moisture. The bones were calcinated at 750°C (see supplementary Figure 1a) and afterwards, the furnace was switched off to allow the samples to cool naturally. The heat treatment helped to decompose the organic matter, change the color of the bones to white and produce lime. The bones were milled using a Retsch planetary ball mill and dry sieved using 90 µm to form a white powder (see supplementary Figure 1b). The mesh size used for all the raw materials was chosen based on a previous study that reported that such particles exhibit enhanced strength and dielectric properties [9,13].

Sample formulation

Porcelain insulators are made following three basic steps that include mixing, pressing and firing. The powder samples were mixed in proportions shown in supplementary Table 1. As seen, feldspar was replaced with CBA in a range of 0-25 wt%. The other materials such as ball clay, kaolin and sand were kept constant at 20 wt%, 30 wt% and 25 wt% respectively. The aim was to evaluate the effect of replacing feldspar with CBA on the dielectric and mechanical strength of porcelain insulators formed. Formulation 1 with 25 wt% feldspar and 0 wt% CBA was considered as the control sample while formulations 2 to 5 (see supplementary Table 1) were experimental samples. Each formulation was homogenized for 20 minutes using an electrical hand mixer (model, GHM6127200W). A moisture content of 15 wt. % was added and the mixture was homogenized further for 20 minutes. Afterwards, 50 g of the powder mixture was poured in a cylindrical steel mould where a uniaxial pressure of 40 MPa was applied. Cylindrical disks measuring 10 mm thick and 50 mm in diameter were formulated. For each peak temperature, ten (10) samples were produced totaling to fifty (50) samples for all the peak temperatures considered. The green body was air dried to avoid cracks due to residual stress. Studies have shown that feldspar starts to melts into a molten phase at 980 °C, and it ends at approximately 1200 °C [22]. On this basis, the samples were fired at peak temperature of 1000, 1050, 1100, 1200 and 1250°C. The firing process was carried out at rate of 6°C/min and a dwell time of 2 hrs using Carbolite muffle furnace. [Fig. 1\(a\)](#) shows the appearance of porcelain insulators after firing. However,

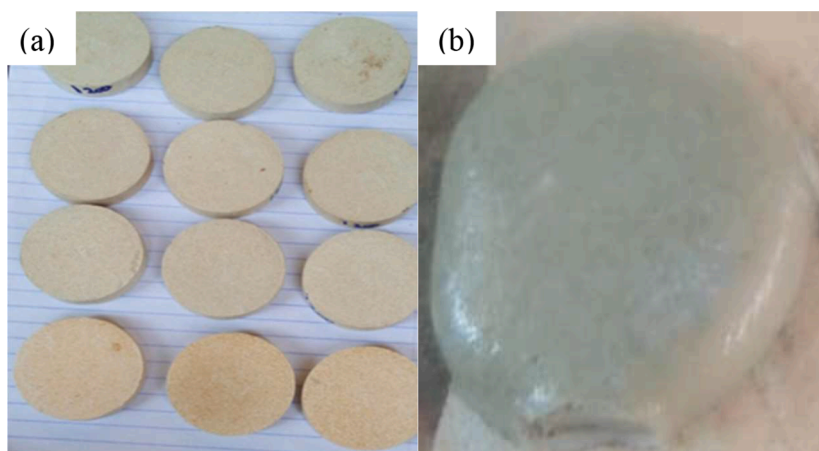


Fig. 1. (a) Dimensionally stable samples fired in a range of 1000-1250 °C, (b) dimensionally unstable samples fired at 1300 °C.

samples fired at 1300 °C exhibited dimensional breakdown as illustrated in Fig. 1(b), and they were not considered for experimental analysis.

Characterization of samples

The chemical composition of the raw materials was carried out using X-ray fluorescence (XRF) method and the results are presented in Table 1. Phase and microstructure analysis of the fired samples was studied using X-ray diffractometer and scanning electron microscope (SEM) respectively. The phases present in the fired samples were analyzed using an X'pert PRO PANalytical X-ray diffractometer, PW 3050/60, with Ni-filtered K ~ Cu-radiation generated by a 40 kV acceleration voltage and a 40 mA anode current. Pulverized specimens were scanned from 10 to 60° operating the equipment at a 2θ scan speed of 0.5 s/step and a 2θ step size of 0.02°. The X-ray peaks were identified using the software of the instrument and the results are presented in Fig. 2.

FEG-SEM instrument, ZEISS LEO 1530 with a GEMINI column was used to analyze the microstructure of the fired samples. Here, sectioned and polished specimens were used for the investigation and the results are presented in Fig. 3. The specimens were polished, cleaned and dried. Thereafter, they were dipped in 40% concentrated hydrochloric acid for 25s, cleaned, dried and studied using FEG-SEM instrument. The cleaning procedures given to all specimens before examination included washing in water and alcohol before drying.

Experimental analysis

Dielectric strength

The dielectric strength of the fired samples was tested using the insulating oil dielectric strength tester. The procedure used was based on the ASTM D149 standard for testing the dielectric strength of porcelain insulators [23]. Testing was carried out at room temperature and relative humidity of 77.2%. The samples tested were placed between two (2) spherical electrodes measuring 20 mm each in diameter (D). The distance between electrodes (S) was 8 mm, and since $S \leq 0.5D$, the distribution of electric fields across electrodes during measurement was uniform. The power supply was turned on and the test voltage was gradually increased from 0 kV at a rate of 2 kV/s to eliminate any thermal effects. The failure of the sample was noticed by a spark across the electrodes and the maximum voltage at this point was noted and recorded as V_{BD} . Prior to the measurement, electrodes and samples were carefully polished to eliminate any surface defects. Further, the samples were submerged in transformer oil to avoid any flash overs. For each peak temperature and formulation (see supplementary Table 1), a total of five (5) samples were tested and the average voltage breakdown value, including the standard deviation was calculated. The dielectric strength (δ_{DS}) was calculated using Eq. (1) [13].

$$\delta_{DS} = \frac{V_{BD}}{h}, \quad (1)$$

where h is the thickness of the ceramic insulator measured using Vernier caliper in millimeters.

Mechanical strength

Flexural strength of the samples was determined based on 3 point loading method using Testometric Material Testing Machine. The

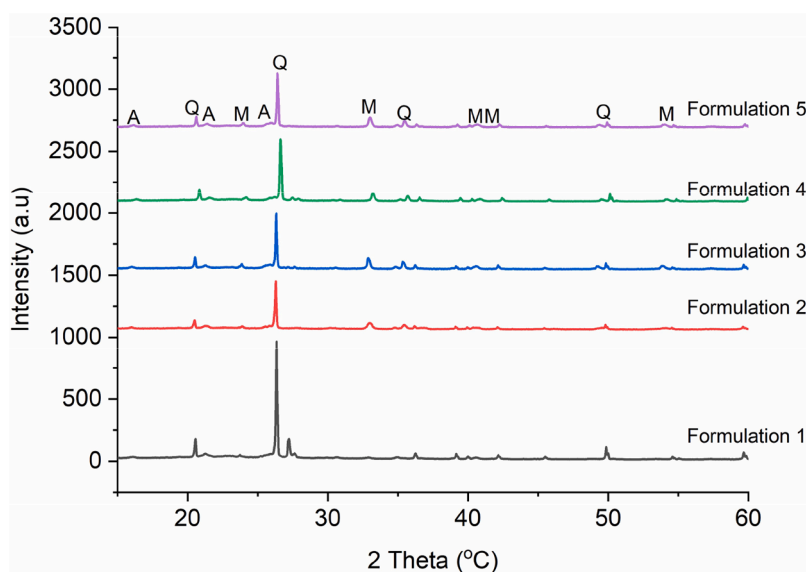


Fig. 2. XRD patterns for samples fired at 1250 °C.

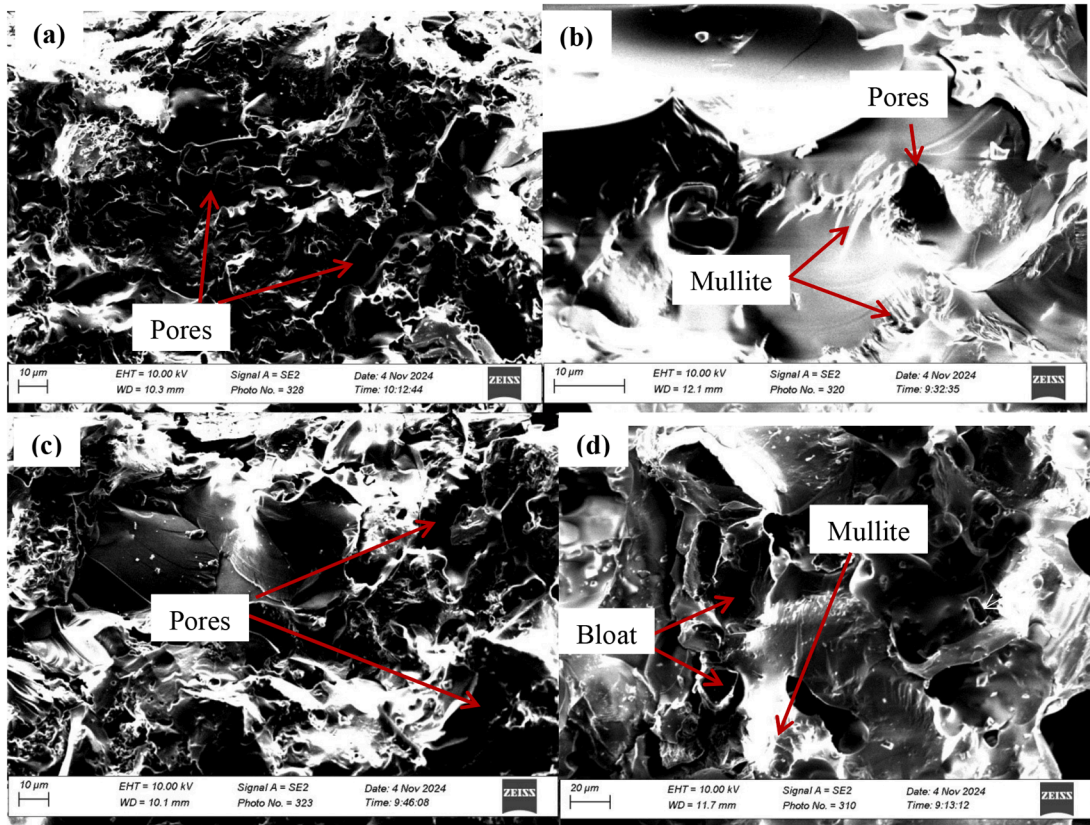


Fig. 3. SEM images; (a) formulation 1 fired at 1000°C, (b) formulation 1 fired at 1250°C, (c) formulation 5 fired at 1000°C and (d) formulation 5 fired at 1250°C.

test was performed on cylindrical disks (height = 10 mm x diameter = 50 mm). The sample was fixed between two supports and a crosshead speed of 3 mm/min was applied until fracture. The breaking force (F_{fr}) was recorded, a total of five (5) samples were considered at each peak temperature, their average as well as standard deviations was computed. Flexural strength (σ_f) was calculated using Eq. (2) [13].

$$\sigma_f = \frac{2F_{fr}}{\pi Dh}, \quad (2)$$

where D is the diameter of the sample measured using a vernier caliper in millimeters.

Results and discussion

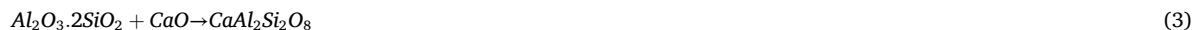
Characterization of the samples

Chemical composition

Porcelain insulators were prepared from cattle bone ash, kaolin, ball clay, feldspar and sand. The chemical composition of the starting raw materials as determined by X-ray fluorescence method is shown in Table 1. The results show that CaO (71%), and Si₂O (16%) were the major oxides present in CBA. This indicated a high content of the fluxing oxide (CaO) in CBA, a similar observation was reported by Abdulwahab et al. [20]. Other oxides (Fe₂O, K₂O, Na₂O, MgO, ZnO and Ni₂O) totalized < 6 %. The chemical composition of feldspar revealed Si₂O (68%), K₂O (19%) and Al₂O₃ (8%) as the main oxides, other oxides existed in minor quantities. Due to the high content of K₂O in feldspar, it was classified as orthoclase and therefore it enabled a broader firing range. The ratio of Al₂O/SiO₂ in kaolin was comparable to the theoretical ratio of pure kaolinite which is 1:2, this was remarkable for mullite phase formation during sintering [24,25]. Sand constituted 86% silica which was low compared to 95 % reported elsewhere [12]. Sand was used to maintain the dimensional stability of the fired products. However, samples fired at 1300 °C exhibited dimensionally failure (Fig. 1b). This could be attributed to the purity of sand used. Fe₂O₃ and TiO₂ constituted 13% and 2% in ball clay respectively. These oxides influence the coloration of fired product. For white ware, the amount of ball clay in the mixture should not exceed 15 wt%. In addition, the amount of Fe₂O₃ should be less than 3 % [9,26]. This explains the color of the fired products (Fig. 1a). The raw materials used were found to be suitable for the production of porcelain insulators.

Phase analysis

The XRD patterns of formulations 1 to 5 after firing at 1250 °C is shown in Fig. 2. Quartz (labeled as Q), mullite (labeled as M) and anorthite (labeled as A) appear as the major crystalline phases in the fired samples. The peaks at $2\theta \approx 15^\circ$ - 28° (JCPDS card number 41-1486) were inherent to anorthite crystalline phase. It suggests that the glassy matrix was rich in anorthite ($\text{CaAl}_2\text{Si}_2\text{O}_8$). The formation of the glassy phase was due to the reaction between metakaolin ($\text{Al}_2\text{O}_3 \cdot 2\text{SiO}_2$) from the kaolinitic clay relics and lime (CaO) via Eq. (3). The presence of anorthite was attributed to the high amount of CaO in CBA (Table 1) [21].



The quartz (SiO_2) phase at $2\theta \approx 26.6^\circ$, 20.8° , 35.6° and 50.3° were matched with JCPDS card number 898935. The mullite phase ($2\text{Al}_2\text{O}_3 \cdot 3\text{SiO}_2$) at $2\theta \approx 24.5^\circ$, 33.2° , 39.2° , 40.8° and 54.6° was matched with JCPDS card number 150776. The mullite phase was formed by the decomposition of kaolinite relics and the melt during sintering [27]. The intensity of peaks for samples with CBA (formulations 2 - 5) is similar. It indicates that the crystalline phases formed are in equal proportions in the fired samples. In comparison, the intensity of the peaks in samples without CBA (formulation 1) for quartz is higher than the ones with CBA hence more quartz grains are present in CBA samples. The mullite peaks appear higher in samples with CBA than those without. This means that the quantity of mullite fibers in the samples with CBA exceeds those without CBA. The presence of the crystalline phases influence both the dielectric and mechanical strength of the fired product [1].

Microstructure analysis

The SEM analysis for compositions 1 and 5 after sintering at 1000 °C and 1250 °C was carried out, and the results are presented in Fig. 3. The micrographs revealed differences in surface morphology with firing temperature and CBA ratios. In samples with 0 wt% CBA (formulation 1) fired at 1000 °C, larger and interconnected pores were formed as seen in Fig. 3a. At 1250 °C, smaller, spherical and more isolated pores were exhibited which indicated liquid phase sintering mechanism. The mullite fibers in their needle-like morphology, embedded in a glassy like matrix can be seen in Fig. 3b. Fig. 3c illustrates SEM micrograph for samples with 25 wt% CBA after firing at 1000 °C. The images appeared to show a glassy like surface morphology with small and less connected pores. The presence of glassy like substances at low temperature was attributed to the high amount of CaO in CBA (Table 1) [3]. At 1250 °C, the mullite fibers were present (Fig. 3d), formed due to crystallization of aluminosilicate relics. In addition, the formation of secondary pores also called bloats (see Fig. 3d) was attributed to high amount CaO and Fe_2O_3 (13%) in the raw materials (see Table 1) [16,28].

Experimental analysis

Dielectric and flexural strength are the two most important properties of porcelain insulators for electrical application [29].

Dielectric strength

Dielectric strength was evaluated as a function of firing temperature and CBA ratios, and the results are presented in Fig. 5 (a-e). The dielectric strength for samples with 0 wt% CBA increased from 11 to 15 kV/mm with temperature, see Fig. 5a. A similar observation was reported by Merga et al. [25]. The increase was attributed to phase evolutions (Fig. 3) [13]. An increase in firing temperature raises the population of mullite fibers and the volume of the glassy phase. The mullite fibers are insulators in nature, and their low dielectric constant of 5 - 6 at a frequency of 1kHz contributes to a high dielectric breakdown [8]. The glassy phase on the other hand diffuses into the open pores increasing the vitrification of the material. This reduces the areas (pores) where electric fields would pill up hence increasing dielectric strength. In an excess amount however, the glassy phase has a detrimental effect on the dielectric strength of the material [9,25].

Addition of CBA in a range of 5-10 wt% (formulations 2 and 3) showed a non-monotonic trend. In samples with 5 wt% CBA, a slight decline from 12.7 to 12.3 kV/mm in dielectric strength with temperature was exhibited. Further increase in temperature to 1100 °C resulted in a sharp increase in dielectric strength to 15 kV/mm. At 1250 °C, the dielectric strength reduced to 11 kV/mm (Fig. 5b). In samples with 10 wt.% CBA, dielectric strength increased from 12.8 to 14.9 kV/mm at temperatures of 1000 to 1050 °C, a further increase in temperature resulted in a decline in the dielectric strength as shown in Fig. 5c.

In contrast, addition of CBA in a range of 20-25 wt% (formulations 4 and 5) resulted in a decline in dielectric strength with temperature as illustrated in Fig. 5d and e. The dielectric strength of the samples with 25 wt% CBA (formulation 5) was measured as 15 kV/mm, after firing at 1000 °C. The low firing temperature was attributed to high content of CaO in CBA (Table 1). Earth alkali oxides such as CaO lowers the melting temperature of silica, leading to an early formation of the glassy phase [22]. The glassy phase promotes vitrification by closing up the interconnected pores as evident in Fig. 3c hence, increasing the dielectric strength. On the same note, a dielectric strength of 15 kV/mm was achieved by samples with 0 wt% CBA after firing at 1250 °C. It indicated that adding CBA (25 wt%) reduces the firing temperature of the insulators by about 250 °C. The firing temperature in this case was the temperature when the dielectric strength was at maximum. Gouvea et al. [16] reports a reduction in firing temperature of 50 °C when 2 wt% of bone ash was added to clay, feldspar and sand. A similar observation is reported in ref. [21].

Furthermore, an increase in firing temperature to 1250 °C for samples with CBA (25 wt%) resulted in a decline in dielectric strength to 8 kV/mm as shown in Fig. 5e. The decline in dielectric strength was attributed to the formation of excess amount of the glassy phase during firing. As mentioned before, the high content of CaO in CBA forms eutectics that lower the melting temperature of silica consequently forming glassy phase at an early stage [3]. It is expected that at high temperatures, an excess amount of the glassy phase was produced. The presence of a large amount of the glassy phase is detrimental to the dielectric strength of the insulator [30].

Increasing the amount of CBA (CaO) increases the concentration of non-bridging oxygen (NBO) in the glassy matrix [31]. Fig. 4 illustrates the transformation of bridging oxygen (BO) to NBO and tricluster oxygen (T).

The presence of NBO and T creates a weak bond between the tetrahedral ion Al^{3+} or Si^{2+} with one or more modifier ion (Ca^{2+} , K^+ etc) [31]. In excess amount, the glassy phase ($CaAl_2Si_2O_8$) acts as a transport medium for the free ions (Al^{3+} etc.) [9,25]. The high ion mobility reduces the dielectric breakdown of the insulator.

CaO reduces the temperature when liquid phase formation occurs in porcelains. At a firing temperature of 1250 °C, the volume of the liquid phase increases and its corresponding viscosity reduces [32]. Iron oxide (see Table 1) decomposes at high temperatures releasing oxygen gas via Eq. (4) [28,33].



The escape of entrapped oxygen gas from the glassy matrix resulted in the formation of secondary pores called bloats as seen in Fig. 3d. Gouvea et al. [16] reports a similar defect in porcelain bodies containing CaO at firing temperature of 1200 °C. The bloats act as sites where electric fields accumulate [30] thus, reducing the voltage breakdown of the insulator. In this study, all the samples containing CBA, fired in a range of 1000-1250 °C exhibited values of dielectric strength within or above the range of 6-13 kV/mm which is specified range for porcelain insulators [1,8,9].

Mechanical strength

Mechanical (flexural) strength is among the major parameters used in the classification of porcelain insulators. It determines the ability of the insulator to withstand harsh conditions without failure. Flexural strength increased with firing temperature (1000-1250 °C) in samples with 0 wt% CBA (Fig. 6a). A similar observation is reported in ref. [34]. At low firing temperatures of less than 1100°C, the formation of the glassy phase was limited consequently, vitrification was not well facilitated [35]. This is evident by the interconnected network of pores (Fig. 3a), which results from low vitreous phase formation during liquid state sintering. As a result, the samples exhibited flexural strength of 9.8-10.7 MPa. At 1250 °C, flexural strength of 28.8 MPa was obtained, a similar trend was observed when 5 wt% CBA was added (Fig. 6b). The increase in flexural strength was attributed to vitrification of the samples facilitated by liquid phase sintering. This is evident in Fig. 3b where the interconnected pores were blocked by the glassy phase. The increase in flexural strength was also attributed to mullitization of the samples as evident in Figs. 2 and 3b. The feltlike interlocking of the mullite fibers at higher temperatures is responsible for porcelain strength according to the mullite hypothesis [11,36].

The transformation of kaolinitic relics (clay and feldspar see Table 1) into mullite fibers during firing occurs in stages. At a firing temperature of 450-650 °C, kaolinite ($Al_2SiO_5(OH)_4$) transforms into amorphous metakaoline (Al_2SiO_7) and water via Eq. (5). At temperatures beyond 1100 °C, metakaoline transforms into crystalline mullite fibers ($3Al_2O_3 \cdot 2SiO_2$) and amorphous silica (SiO_2) via Eq. (6) [9]. The population of mullite and the interlocking behavior of the fibers increases with firing temperature, enhancing flexural strength of the material [26].



High flexural strength of 38.0 to 38.8 MPa was obtained in samples containing more than 10 wt% CBA after firing at 1250 °C (Fig. 6c-e). Alkali earth oxides such as CaO present in CBA (Table 1) enhances the crystallization of SiO_2 and Al_2O_3 into mullite fibers [32]. The high amount of CaO (71%) present in CBA when added to clay, feldspar and sand enhances the concentration of non-bridging oxygen and tricluster oxygen in the glassy phase. The tricluster oxygen (T) seen in Fig. 4 act as potential sites where nucleation of mullite fibers starts at low temperature [37]. It is anticipated that at 1250 °C, the population of mullite fibers is high in samples with CBA and they interlock efficiently, leading to high flexural strength. The presence of the secondary pores (bloats) had a limited influence on flexural strength as compared to dielectric strength. This was probably attributed to their nature, less interconnected and isolated [33].

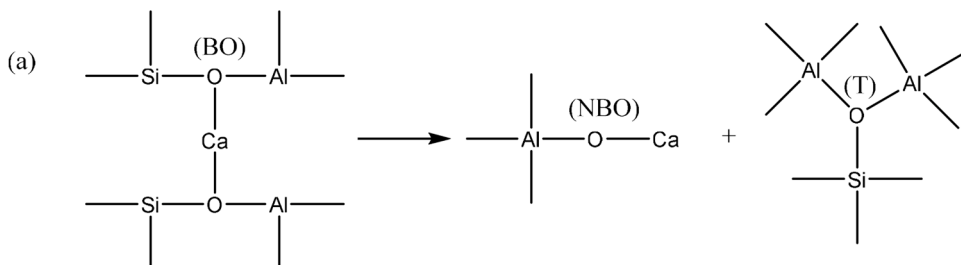


Fig. 4. Transformation of bridging oxygen to non-bridging oxygen and tricluster oxygen[31].

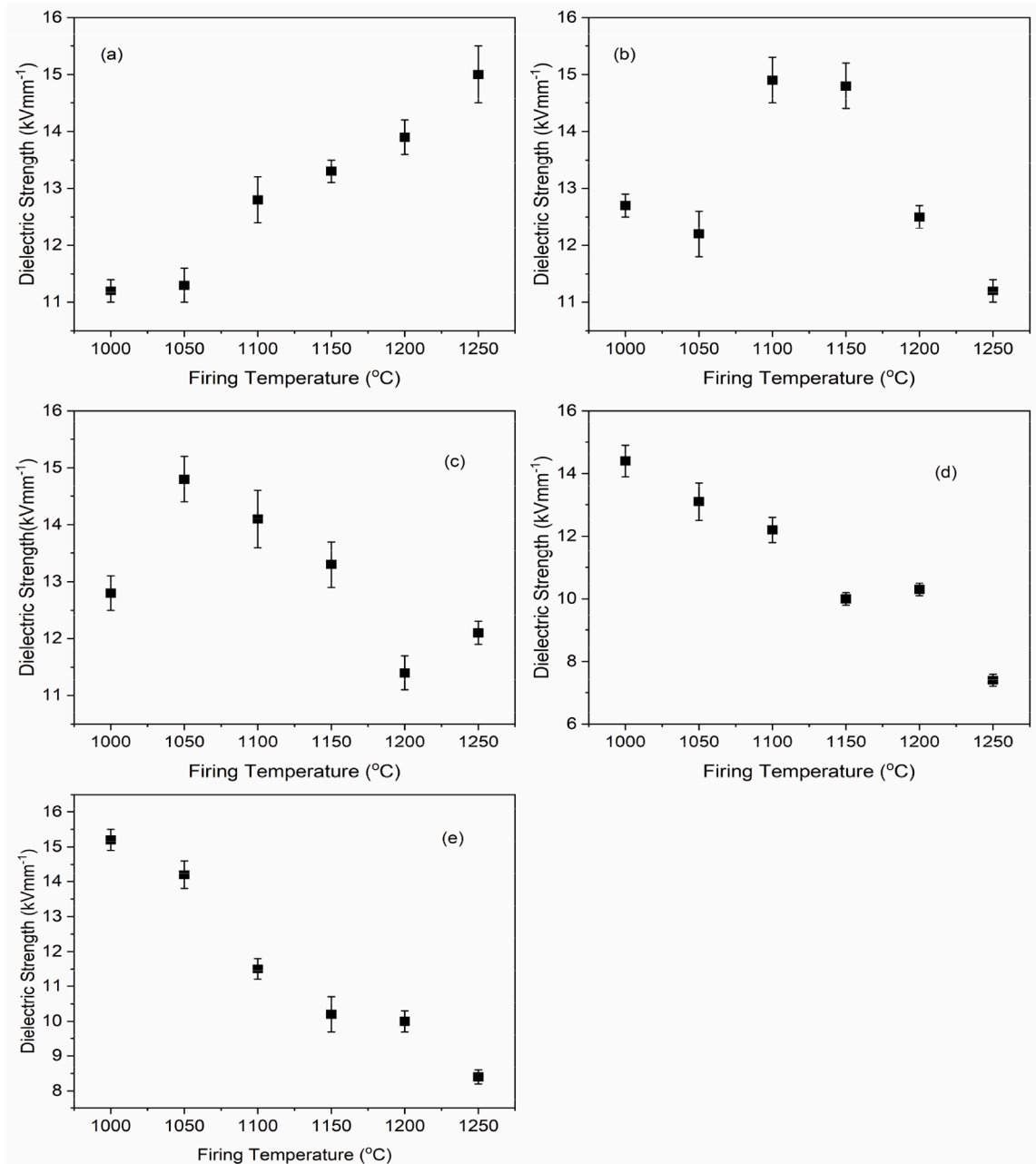


Fig. 5. Dielectric strength of porcelain insulators fired at different temperatures; (a) formulation 1, (b) formulation 2, (c) formulation 3, (d) formulation 4 and (e) formulation 5.

Statistical analysis

The influence of CBA ratio and firing temperature on the dielectric and flexural strength of porcelain insulators was analyzed using design expert software version 13. The response surface methodology (RSM) of central composite design (CCD) was applied. The CBA ratio and firing temperature were considered as factors, the dielectric and flexural strength were the responses in CCD. The responses were determined experimentally using Eqs. (1) and (2). The CBA ratios of 0-25 wt% and firing temperatures of 1000-1250°C were applied in CCD. Supplementary Table 2 summarizes the design matrix for the factors and responses. A two factor interaction (2FI) model in RMS was used to analyze the results of the experimental analysis. Eqs. (7) and (8) represent the 2FI models for dielectric and flexural strength respectively in terms of coded components. Code A represents the CBA ratio and B is for the firing temperature. The positive and negative signs represent cooperative and opposing impacts on the responses.

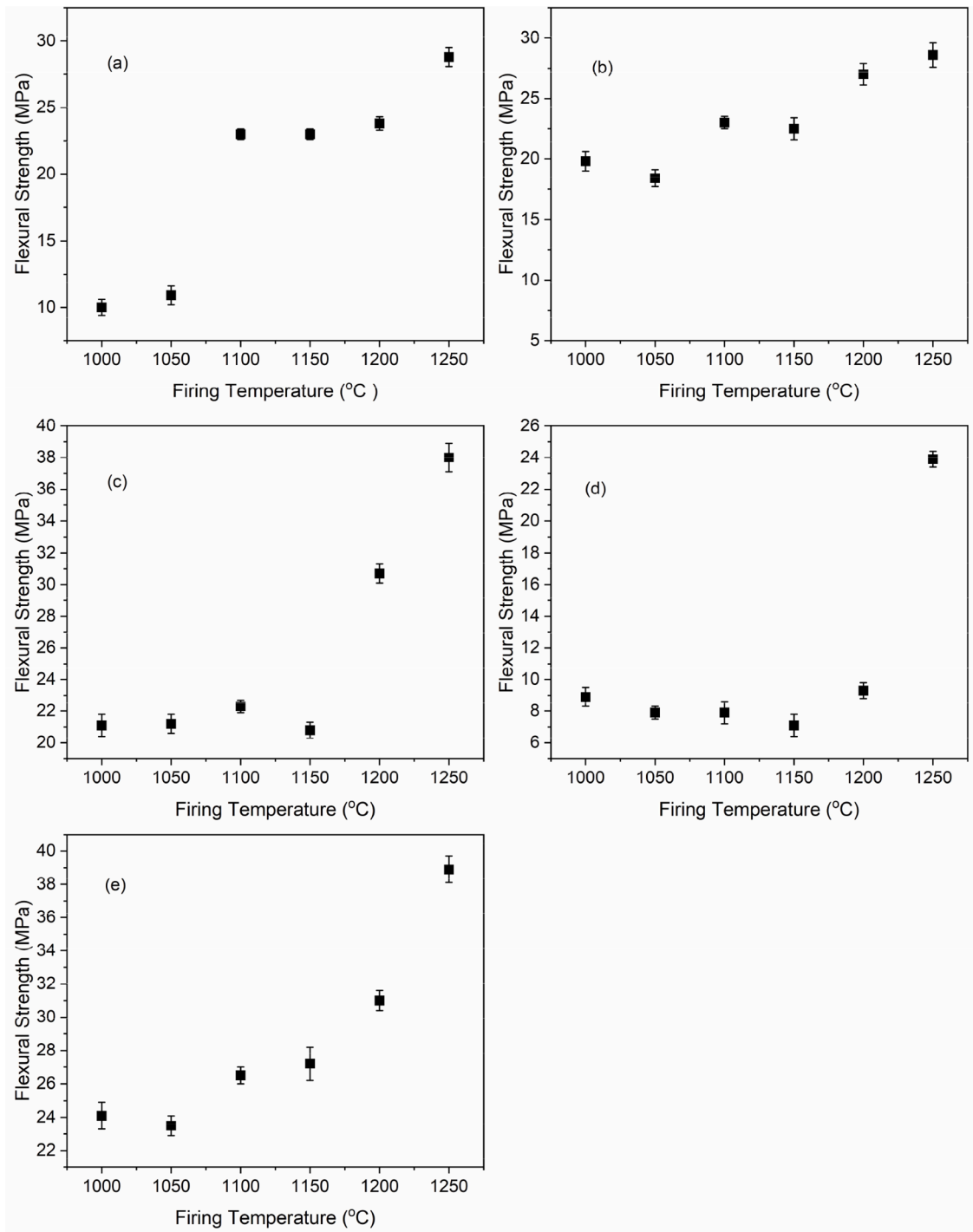


Fig. 6. Modulus of rupture of; (a) formulation 1, (b) formulation 2, (c) formulation 3, (d) formulation 4 and (e) formulation 5 insulators against the firing temperature.

$$\text{Dielectric strength} = 12.59 - 0.77A - 1.33B - 2.17AB \quad (7)$$

$$\text{Flexural strength} = 25.74 + 4.10A + 6.06B + 0.13AB \quad (8)$$

ANOVA for dielectric strength

The dielectric strength analysis of variance is shown in supplementary Table 3 for the 2FI response model. As seen, the predicted value for the response was in agreement with the adjusted value since the difference was less than 2. This means that the correlation between CBA ratio and firing temperature with dielectric strength was strong. The degree of variance between the tested and true value also known as the standard deviation was 1.01 indicating that the model was good [35]. The signal to noise ratio (adeq precision = 13.87) was greater than 4 indicating that the model can be used to identify the optimal configuration [35]. In addition, the model F-value of 13.47 with ($P < 0.05$) implies that there is only a 0.04% chance that F value this large could occur due to noise.

The key model parameters such as A, B and AB were deemed significant ($P < 0.05$). The CBA ratio labeled as A had less significant impact on dielectric strength compared to the firing temperature (B), since its P value was 0.0431 compared to 0.0021 for firing temperature. This is because phase transformations in porcelains was majorly influenced by temperature [36]. Firing from 1000 to 1250 °C resulted in a decline in dielectric strength except for samples with 0wt% CBA (Fig. 5). At 1000 °C, the maximum value of 15 kV/mm was achieved, and this value reduced to 8 kV/mm at 1250 °C after adding 25 wt% CBA. The decline in dielectric strength was attributed to excessive amount of the glassy phase [25,38].

ANOVA for flexural strength

The ANOVA was used to evaluate the statistical significance of the factors of the 2FI model for flexural strength and the results are presented in supplementary Table 4. The predicted and adjusted values agree because their difference is less than 2. This means that both CBA ratio and firing temperature have a strong correlation with flexural strength. From the Table, the standard deviation of 2.9 indicates that the model was good. The adeq precision of 13.72 is greater than 4, meaning that the model can be used to analyze the possible solutions to identify the optimal configuration [35]. The model F-value of 18.83 means that there is only 0.01% chance that an F-value of this magnitude could occur due to noise ($P < 0.0001$) hence indicating that the model is significant. However, for P values greater than 0.05 the model terms are insignificant and therefore reduction may improve the model. Firing temperature had a significant effect ($P < 0.0001$) than CBA ration ($P = 0.0014$) on flexural strength of porcelain insulators. The reason was that phase transformation such as glassy phase and mullite formation are majorly influenced by temperature changes [11].

Optimization of factors and responses

The CBA ratio in feldspar chosen during the optimization process was in a range of 0-25 wt%, and the firing temperature was 1000-1250 °C. The desirability function in RMS was used to obtain the optimum conditions for factors and responses. Supplementary Figure 2 shows contour plots for the factors and the responses at optimal conditions. The desirability function which determines the best conditions for the prediction of the factors and the responses is shown in supplementary Figure 2. According to Yiga et al. [39], the desirability which approximates to 1, means that the conditions obtained are very good. The optimal conditions of the factors were 10 wt% of CBA and firing temperature of 1039 °C. The corresponding responses were 13 kV/mm and 22 MPa for dielectric and flexural strength respectively (see supplementary Figure 2a and b). The experimental results at optimal conditions indicated a dielectric and mechanical strength of 15 kV/mm and 24 MPa respectively at a firing temperature of 1000 °C with 25 wt% CBA. It indicates that high values of dielectric strength specified for electrical insulators (6-15 kV/mm) can be realized at low temperature when CBA is added as a fluxing material in porcelain insulators.

Conclusions

Cattle bone ash was found to contain a high content of CaO, it was suitable for use as a fluxing material in porcelain insulators. CBA was added in a range of 0-25 wt% as a replacement of feldspar. After mixing with kaolin, ball clay and sand, the samples were fired in a range of 1000-1250 °C. In samples with 0 wt% CBA, increasing temperature resulted in an increase in the dielectric strength of the insulators. A maximum dielectric strength of 15 kV/mm was achieved at 1250°C. When CBA was added, the dielectric strength reduced with temperature. At 1000 °C, a dielectric strength of 15 kV/mm was recorded in samples with 25 wt% of CBA. At optimal conditions using RSM, a dielectric strength of 13 kV/mm with 10 wt% CBA at a firing temperature of 1040 °C was achieved. It indicates that, using CBA lowers the firing temperature required to obtain a maximal dielectric strength. As a result, energy is saved during the production process. In all the samples containing CBA, the dielectric strength was within the specification of 6-15 kV/mm recommended for porcelain insulators. This work therefore, demonstrated that cattle bone ash can be used to replace feldspar as a raw material in the production of porcelain insulators

Funding statement

There are no sources of funding to declare.

Data availability

Data supporting these findings are available within the article or upon request.

Credit author statement

Ritah Abindabyamu: characterized the raw materials, experimental analysis, and reviewed the manuscripts. **Eneku John Paul:** reviewed the manuscript. **William Ochen:** study conceptualization, drafted the original manuscript, data analysis. All authors read and approved the final manuscript.

Declaration of competing interest

The authors declare that they have no known competing financial interests to declare.

Supplementary materials

Supplementary material associated with this article can be found, in the online version, at [doi:10.1016/j.sciaf.2026.e03428](https://doi.org/10.1016/j.sciaf.2026.e03428).

References

- [1] E. Beyene, S.N. Tiruneh, D.M. Andoshe, A.M. Abebe, Partial substitution of feldspar by alkaline-rich materials in the electrical porcelain insulator for reduction of processing temperature, *Mater. Res. Express* 9 (6) (2022), <https://doi.org/10.1088/2053-1591/ac7301>.
- [2] M.L. Sall, A.K.D. Diaw, D. Gningue-Sall, S. Efremova Aaron, J.J. Aaron, Toxic heavy metals: impact on the environment and human health, and treatment with conducting organic polymers, a review, *Environ. Sci. Pollut. Res.* 27 (24) (2020) 29927–29942, <https://doi.org/10.1007/s11356-020-09354-3>.
- [3] M. Yousaf, et al., Microstructural and mechanical characterization of high strength porcelain insulators for power transmission and distribution applications, *Ceram. Int.* 48 (2) (2022) 1603–1610, <https://doi.org/10.1016/j.ceramint.2021.09.239>.
- [4] A. Olad, F. Maryami, A. Mirmohseni, A.A. Shayegani-Akmal, Potential of slippery liquid infused porous surface coatings as flashover inhibitors on porcelain insulators in icing, contaminated, and harsh environments, *Prog. Org. Coatings* 151 (December 2020) (2021) 106082, <https://doi.org/10.1016/j.porgcoat.2020.106082>.
- [5] K. Raj, A.P. Das, Lead pollution: impact on environment and human health and approach for a sustainable solution, *Environ. Chem. Ecotoxicol.* 5 (February) (2023) 79–85, <https://doi.org/10.1016/j.eneco.2023.02.001>.
- [6] M. Balat, Electricity from worldwide energy sources, *Energy Sources, Part B Econ. Plan. Policy* 1 (4) (2006) 395–412, <https://doi.org/10.1080/15567240500400879>.
- [7] L. Lu, Q. Weng, Y. Xie, H. Guo, Q. Li, An assessment of global electric power consumption using the defense meteorological satellite program-operational linescan system nighttime light imagery, *Energy* 189 (xxxx) (2019) 116351, <https://doi.org/10.1016/j.energy.2019.116351>.
- [8] P.W. Olupot, S. Jonsson, J.K. Byaruhanga, Development and characterisation of triaxial electrical porcelains from Ugandan ceramic minerals, *Ceram. Int.* 36 (4) (2010) 1455–1461, <https://doi.org/10.1016/j.ceramint.2010.02.006>.
- [9] A. Merga Tullu, et al., Effect of cullet on firing temperature and dielectric properties of porcelain insulator, *Heliyon* 8 (2) (2022) e08922, <https://doi.org/10.1016/j.heliyon.2022.e08922>.
- [10] M. Zamani, et al., Investigating the production quality of electrical porcelain insulators from local materials investigating the production quality of electrical porcelain insulators from local materials, *Mater. Sci. Technol.* 413 (2018) 012076, <https://doi.org/10.1088/1757-899X/413/1/012076>.
- [11] W. M. Cam and U. Senapati, "Porcelain-Raw materials, processing, phase evolution, and mechanical behavior," no. 190529, 1997.
- [12] W. Ochen, F.M. D'ujanga, B. Oruru, Influence of residual stress on the mechanical behavior of ceramics with various quartz sizes, *Sci. African* 11 (2021) e00648, <https://doi.org/10.1016/j.sciaf.2020.e00648>.
- [13] M.F. Al-Hilli, K.T. Al-Rasoul, Influence of glass addition and sintering temperature on the structure, mechanical properties and dielectric strength of high-voltage insulators, *Mater. Des.* 31 (8) (2010) 3885–3890, <https://doi.org/10.1016/j.matdes.2010.02.048>.
- [14] K. Belhouchet, A. Bayadi, H. Belhouchet, M. Romero, Improvement of mechanical and dielectric properties of porcelain insulators using economic, *Boletín la Soc. Española Cerámica y Vidr* 58 (1) (2019) 28–37, <https://doi.org/10.1016/j.bsecv.2018.05.004>.
- [15] M. Shanmugam, G. Sivakumar, A. Arunkumar, D. Rajaraman, M. Indhira, Fabrication and assessment of reinforced ceramic electrical insulator from bamboo leaf ash waste, *Elsevier B.V.*, 2020, <https://doi.org/10.1016/j.jallcom.2020.153703>.
- [16] D. Gouvêa, T. Tisse, H. Kahn, E. De Souza, Using bone ash as an additive in porcelain sintering, *Ceram. Int.* 41 (1) (2015) 487–496, <https://doi.org/10.1016/j.ceramint.2014.08.096>.
- [17] G.I. Samuel, J.O. Atiba, O.S.I. Fayomi, Next Sustainability Synergistic mechanical and environmental performance of cow bone ash-brass dross hybrid composites for ceiling applications, *Next Sust.* 6 (August) (2025) 100179, <https://doi.org/10.1016/j.nxsust.2025.100179>.
- [18] A.D. Omah, B.A. Okorie, E.C. Omah, I.C. Ezema, V.S. Aigbodion, Measurement of dielectric properties of polymer matrix composites developed from cow bone powder, *Int. J. Adv. Manuf. Technol.* 88 (2017) 325–335, <https://doi.org/10.1007/s00170-016-8759-1>.
- [19] J.O. Akindoyo, S. Ghazali, M.D.H. Beg, N. Jeyaratnam, Characterization and elemental quantification of natural hydroxyapatite produced from cow bone, *Chem. Eng. Technol.* 42 (9) (2019) 1805–1815, <https://doi.org/10.1002/ceat.201800636>.
- [20] R. Abdulwahab, B.D. Ikotun, A.A. Raheem, E.A. Adetoro, R. Salihu, O.A. Oribamise, Effects of cow bone ash as a partial replacement of cement in the production of concrete, *J. Build. Pathol. Rehabil.* 10 (2) (2025), <https://doi.org/10.1007/s41024-025-00627-3>.
- [21] R. Sokolář, L. Kersnerová, M. Svěda, The effect of different fluxing agents on the sintering of dry pressed porcelain bodies, *Integr. Med. Res.* 5 (3) (2017) 290–294, <https://doi.org/10.1016/j.jascer.2017.06.001>.
- [22] Y. Iqbal, P.F. Messer, W.E. Lee, Microstructural evolution in bone china, *Br. Ceram. Trans.* 99 (5) (2000) 193–199, <https://doi.org/10.1179/096797800680938>.
- [23] L. Bhanuprakash, S. Varghese, S.K. Singh, Glass fibre reinforced epoxy composites modified with graphene nanofillers : electrical characterization, *J. Nanomater.* (1) (2022) 4611251, <https://doi.org/10.1155/2022/4611251>.
- [24] R.G. Frizzo, A. Zaccaron, V. de Souza Nandi, A.M. Bernardin, Pyroplasticity on porcelain tiles of the albite-potassium feldspar-kaolin system: a mixture design analysis, *J. Build. Eng.* 31 (April) (2020) 101432, <https://doi.org/10.1016/j.jobe.2020.101432>.
- [25] A. Merga, H.C.A. Murthy, E. Amare, K. Ahmed, E. Bekele, Heliyon Fabrication of electrical porcelain insulator from ceramic raw materials of Oromia region, Ethiopia, *Heliyon* 5 (March) (2019) e02327, <https://doi.org/10.1016/j.heliyon.2019.e02327>.

- [26] W. Ochen, F.M. D'ujanga, B. Oruru, P.W. Olupot, Physical and mechanical properties of porcelain tiles made from raw materials in Uganda, *Results Mater.* 11 (2021) 100195, <https://doi.org/10.1016/j.rinma.2021.100195>.
- [27] T.K. Mukhopadhyay, S. Ghosh, J. Ghosh, S. Ghatak, H.S. Maiti, Effect of fly ash on the physico-chemical and mechanical properties of a porcelain composition, *Ceram. Int.* 36 (3) (2010) 1055–1062, <https://doi.org/10.1016/j.ceramint.2009.12.012>.
- [28] Y. Sawadogo, et al., Porcelain: raw materials, technological properties and applications—a review, *J. Soc. Ouest-Afr. Chim.* 53 (2024).
- [29] T. Ologunwa, et al., Optimizing performance of porcelain insulators : how does particle size influence dielectric and mechanical strengths ? *Acta Mech. Slovaca* 25 (2) (2021) 20–28, <https://doi.org/10.21496/ams.2021.017>.
- [30] L. Boussof, et al., Effect of amount and size of quartz on mechanical and dielectric properties of electrical porcelain, *Trans. Indian Ceram. Soc.* 77 (3) (2018), <https://doi.org/10.1080/0371750X.2018.1500148>.
- [31] S. Mno, P. Rev, J.F. Stebbins, Z. Xu, NMR evidence for excess non-bridging oxygen in an aluminosilicate glass, *Nature* 390 (1997) 1996–1998, <https://doi.org/10.1038/36312>.
- [32] Z.B. Ozturk, N. Ay, Processing Research An investigation of the effect of alkaline oxides on porcelain tiles using factorial design, *J. Ceram. Process. Res.* 13 (5) (2012) 635–640, <https://doi.org/10.36410/jcpr.2012.13.5.635>.
- [33] Y. Kobayashi, O. Ohira, Effect of firing temperature on bending strength of porcelains for tableware, *J. Am. Ceram. Soc.* 75 (7) (1992) 1801–1806, <https://doi.org/10.1111/j.1151-2916.1992.tb07200.x>.
- [34] C.S.O.T.C. Madueme, Manufacture of porcelain insulators from locally available materials, *Electr. Eng.* 102 (2020) 1959–1968, <https://doi.org/10.1007/s00202-020-00998-5>.
- [35] J. Atidi, H. Kasedde, E. Menya, P. Wilberforce, Optimization of physical and mechanical properties of porcelain tiles from coffee parchment husk ash, *J. Eng. Res.* 13 (November) (2025) 820–832, <https://doi.org/10.1016/j.jer.2023.11.013>.
- [36] Z. Bayer Ozturk, Microstructural characterization of mullite and anorthite-based Porcelain tile using regional clay, *J. Ceram. Process. Res.* 17 (6) (2016) 555–559.
- [37] T. Takei, Y. Kameshima, A. Yasumori, and K. Okada, “Crystallization kinetics of mullite from Al₂O₃ – SiO₂ glasses under non-isothermal conditions,” vol. 21, pp. 2487–2493, 2001.
- [38] Y. Xu, C. Lin, J.U.N. Du, Effect of glass-phase design on the dielectric properties of PbO-SrO-Na₂O-Nb₂O₅-SiO₂ glass – ceramic, *J. Electron. Mater.* 44 (11) (2015) 4053–4057, <https://doi.org/10.1007/s11664-015-4009-9>.
- [39] V. Andrew, Y. Michael, S. Pagel, P. Wilberforce, O. Johannes, C. Bonten, Optimization of tensile strength of PLA /clay / rice husk composites using Box - Behnken design, *Biomass Convers. Biorefinery* 13 (13) (2023) 11727–11753, <https://doi.org/10.1007/s13399-021-01971-3>.